

A Comparative Study for Optimum Design of Grid Connected PV System based on Actual System Specifications

M. S. Hassan

Electrical Engineering Department,
Faculty of Engineering, Minia University
El-Minia 61517, Egypt

Adel A. Elbaset

Electrical Engineering Department,
Faculty of Engineering, Minia University
El-Minia 61517, Egypt

ABSTRACT

This paper presents a comparative study using new approach for optimum design of rooftop grid connected PV system installation on an institutional building at Minia University, Egypt. The new approach demonstrated in this paper based on optimal configuration of PV modules along with inverters according to not only MPP voltage range but also maximum DC input currents of the inverter. Five different brands of commercially available PV modules and inverters have been conducted in this study. Many different configurations of rooftop grid connected PV systems have been investigated and a comparative study among these configurations has been carried out taking into account PV modules and inverters specifications. Energy production aptitudes, cost of energy, simple payback time and GHG emissions have been appraised for each configuration using proposed MATLAB computer approach. Simulation results show that, annual energy production of about 258.8 MWh, COE of about 0.5482 \$/kWh, payback period equal 6.95 years and total annual GHG emissions reduction of about 180.9 tons.

General Terms

Design, Programming, Solar Energy.

Keywords

Sizing PV system, Rooftop grid-connected, MPP voltage range, On-grid, Greenhouse Gas, MATLAB.

1. INTRODUCTION

The augmenting environmental problems, such as GHG emissions, acid rain, energy shortage, global warming and excessive use of resources, are accelerating development of renewable energy, particularly for the PV technology. In Egypt, total GHG emissions were estimated at 137.11 Mt of CO₂ equivalent, out of which more than 70% was emitted from energy sector including about 35% attributed to the electricity sector [1]. In the context of addressing environmental issues and climate change phenomena, Egypt signed Kyoto Protocol in 1997 and approved it in 2005. According to the Kyoto Protocol, the developed and industrialized countries are obliged to reduce their GHG emissions by 5.2% in the period of 2008-2012 [2]. To achieve this, many industrialized countries seek to decarbonize electricity generation by replacing conventional coal and fossil fuel fired plants with renewable technology alternatives [3]. The favorable climate conditions of Upper Egypt and recent legislation for employing renewable energy sources provide a substantial incentive for installation of PV systems in Egypt. The long-term security requirement of Egypt is to reduce the dependence on imported oil and natural gas and move towards the use of renewable energy sources. Egypt's current captive-

market electricity structure, with the government being a sole buyer, is not conducive to the rise of a new renewable energy regime. However, a new proposed electricity law, now in the process of being approved. The anticipated new electricity law tackles the issue by providing market incentives for private investors, along with those in renewable energy. Competitive bidding for a determined share of the Egyptian network from renewable energy is supposed to build a guaranteed market demand for renewable bulk-energy producers. Additionally, based on decentralization trend, anticipated new law and market structure, it seems likely that electricity prices will rise considerably, including peak-demand figures. Subsidies, as a policy tool, will be used selectively, especially for low-income and low-consumption residential consumers.

The boundless supply of sunlight and wind and their zero emission power generation become a driving force in the fast growth of PV and Wind systems technology. Unlike the dynamic wind turbine, PV installation is static, does not need strong high towers, produces no vibration, and does not need cooling systems. In addition, it is environmentally friendly, safe, and has no gas emissions [4]. PV systems convert the sun's energy directly into electricity using semiconductor materials. They differ in complexity, some are called "stand-alone or off-grid" PV systems, which signifies they are the sole source of power to supply building loads. Further complicating the design of PV systems is the possibility to connect the PV system generation to the utility "grid connected or on-grid" PV systems, where electrical power can either be drawn from grid to supplement system loads when insufficient power is generated or can be sold back to the utility company when an energy surplus is generated [5]. Based on prior arguments, grid-connected or utility-interactive systems appear to be the most practical application for buildings where the available surface is both scarce and expensive. Grid-connected PV systems currently dominate the PV market, especially in Europe, Japan and USA. With utility interactive systems, the public electricity grid acts as an energy store, supplying electricity when the PV system cannot. An interesting problem associated with PV systems is the optimal computation of their size. The sizing optimization of stand-alone or grid connected PV systems is a convoluted optimization problem which anticipates to obtain acceptable energy and economic cost for the consumer [6]. One of the most suitable policies for introducing rooftop PV systems to the market is Feed-in Tariff mechanism. According to this approach, eligible renewable power producers will receive a set price from their utility for all the electricity they generate and deliver to the grid, where grid interactive PV systems derive their value from retail or displacement of electrical energy generated. The power output

of a PV system depends on the irradiance of Sun, efficiency and effective area of PV cells conducted. Therefore, it is compulsory to choose the optimal size of PV system according to the application. Development of rooftop PV technologies has received much attention and introduction of a subsidy for the system cost and energy production especially in Germany and Japan has encouraged the demand for rooftop PV systems [7], where German PV market is the largest market in the world, and Germany is a leading country in terms of installed PV capacity.

E.D. Mehleri *et al.*[8] presented an optimization based approach for evaluation of renewable energy resources on a Greek residential sector taking into account site energy loads, local climate data, utility tariff structure, characteristics of renewable energy technologies (technical and financial) as well as geographical circumstances. C.O.C. Oko *et al.*[9] presented a design analysis of PV system to supply a Laboratory at the Department of Mechanical Engineering, University of Port Harcourt, Nigeria. Life cycle cost and break-even point analyses were carried out to assess the economic viability of the system. An automated MS Excel spreadsheet was developed for the design and economic analyses of PV system in any other location once the input data are sorted. H. H. El-Tamaly and A. A. Elbaset [10] proposed a computer program to determine optimal design of PV system to be installed at Zâfarana site to supply the load demand. The proposed computer program based on minimization of energy purchased from grid. A. Fernandez-Infantes *et al.*[11] developed a specific computer application for automated calculation of all relevant parameters of the installation, physical, electrical, economical as well as ecological for designing a PV system installation that may be either used for internal electric consumption or for sale using the premium subsidy awarded by the Spanish Government. H. Suryatomo *et al.*[12] presented a method to determine optimal capacities of PV system, battery bank and diesel generator unit according to minimum cost objective functions of system reliability and CO₂ emissions. The optimization method included studying on three different PV technologies: ASE-300 (mc-Si based EFG), Kyocera KC-120 (mc-Si based wafer) and AstroPower AP-120 (thin-film Si). Gong and Kulkarni [13] suggested an optimization method for a grid-connected PV system based on maximizing the utilization of the array output energy and minimizing the electricity power sold to the grid. Hongbo Ren *et al.*[14] dealt with the problem of optimal size of grid-connected PV system for residential application and developed a simple linear programming model for optimal sizing of grid-connected PV system. Hernández *et al.*[15] analyzed the optimal maximum size of PV system for different building types. Samimi *et al.*[16] analyzed the optimal tilt angle and other aspects of PV modules in various climates. However, an economic optimization design tool for optimal PV size based on technology information, current tariffs and policy has not yet been developed. R. Haas *et al.*[17] investigated the socio-economic aspects about an Austrian 200 kWp-rooftop program (100 PV systems with an average capacity of 2.28 kWp) to promote small grid-connected PV systems in Austria. A. Al-Salaymeh *et al.*[4] proposed a design of PV system to produce energy for basic domestic needs. They studied the feasibility of utilizing PV systems in a standard residential apartment in Amman city in Jordan to conduct energy and economic calculations. N. K. Bansal and S. Goel [18] discussed integration of 25 kWp solar PV system in an existing building of cafeteria on the campus of Indian Institute of Technology, Delhi by creating a solar roof covering an area

of about 250 m². The system was found to be optimum if integrated with an angle of 15° tilt with relation to north-south axis, in Delhi's climatic conditions, therefore giving it higher efficiency. A. Mellit *et al.*[19] presented an overview of artificial intelligent-techniques for sizing PV systems: stand-alone, grid-connected, PV-wind hybrid systems, *etc.* Muneer *et al.*[20] proposed an optimization model to facilitate an optimal plan for investment in large-scale solar PV generation projects in Ontario, Canada. Kornelakis and Koutroulis [21] analyzed optimization of grid-connected PV systems using a list of commercially available system devices, they select optimal number and type PV module installation, in such a way that the total net economic benefit achieved during the system's operational lifetime period is maximized. Kornelakis and Marinakis [22] proposed an approach to select the optimal PV installation using Particle Swarm Optimization. Aris Kornelakis [23] presented a multi-objective optimization algorithm based on PSO applied to the optimal design of grid-connected PV systems. This paper presents a new approach for optimum design of rooftop grid-connected PV system on an institutional buildings based on optimal configuration of PV modules and inverters according to not only MPP voltage range but also maximum DC input current of the inverter. Several advantages in applying grid connected PV systems on institutional or governmental buildings were found, some of these are the operational hours of office building coincide with the peak power production time of PV systems, and they do not require additional land use, since the building surface is used to accommodate PV modules on the roof. Also the education benefits that comes with owning buildings with PV system raises the awareness of students about renewable energy and energy efficiency issues

2. PROBLEM FORMULATION

Egypt is experiencing one of its most considerable energy crises for decades. Power cuts in Egypt has escalated in recent years due to the shortage of fuel necessary to run power plants - due to the rapid depletion of fossil fuels and continual instability of their prices - and overconsumption of loads especially in summer season, which negatively affected various levels of social and economic activities. On the other hand, Egypt has some of the highest GHG emissions in the world. To solve problems of power cuts and emissions, Egypt is taking impressive steps to rationalize consumption and optimize the use of electricity in addition to develop and encourage PV system projects that can be deployed on rooftop of institutional and governmental buildings. As a result, Egypt government intends to implement about 1000 of grid-connected PV systems on the roof of governmental buildings. As a case study, this paper presents a new approach for optimum design of 100 kW rooftop grid connected PV system for Faculty of Engineering buildings.

3. SITE DETAILS

In order to ensure acceptable operation at minimum cost, it is necessary to determine the correct size of rooftop PV system taking into account meteorological data, solar radiation and exact load profile of consumers over long periods. These factors will be discussed in the following sections

3.1 Site Description

100 kW grid connected PV system install on rooftop of educational buildings B and C of Faculty of Engineering, Minia University is considered. Faculty of engineering comprises offices, lecture halls, laboratories (computer and engineering equipment). Net roof areas available for buildings B and C are 2100 m² and 3100 m² respectively. Coordinate of

selected site is 28.1014 (28° 6' 5'') °N 30.7294 (30° 43' 46'') °W. Electrification of faculty of engineering is often realized through an electric distribution network via three transformers with rated 1000, 500 and 500 kVA from Middle Egypt for Electricity Distribution Company. Figure 1 shows a Google Earth™ image of the selected site.



Figure 1. Google Earth™ image of Faculty of Engineering buildings' layout.

3.2 Load Data

Firstly, the load demand of faculty of engineering has been gathered. Table 1 provides most electrical appliances used in the faculty, while Table 2 provides energy consumption during a recent year, 2013 which have been taken from Upper Egypt Electricity Distribution Company. These values actually gotten from electricity bills paid by the university, where university is the largest customer of its energy supplier. According to energy bills, it was noticed that energy consumed continues to increase due to the increasing loads that faculty added during the recent period. Also it was found that the faculty pays 25 piaster/kWh (3.57 cent/kWh) up to 2012 year as an energy tariff, it is considered as power service on low voltage according to the tariff structure of the Egyptian Electricity Holding Company. Starting from January, 2013 the energy tariff increased by about 13.8% to be 29 piaster/kWh (4.14 cent/kWh). It is expected that, tariff structure continues to increase to reduce governmental subsidies.

Table 2. Typical energy consumption in the faculty for a recent year (2013)

Month	Jan.	Feb.	March	April	May	June	July	Aug.	Sept.	Oct.	Nov.	Dec.	Yearly
Energy (MWh)	71.88	54.78	50.04	67.44	62.04	76.26	80.40	97.44	110.278	98.46	113.76	105.04	980.33

Table 3. Monthly average climate data (kW/m²/day) for El-Minia, Egypt

Month	Jan.	Feb.	March	April	May	June	July	Aug.	Sept.	Oct.	Nov.	Dec.
Radiation (kW/m ²)	4.7	5.78	6.58	7.87	8.03	8.25	7.9	7.70	7.20	6.50	5.59	4.77
Temp., T (C°)	14.3	16.9	17.95	34.3	23.7	30.15	33.3	30.6	31.1	26.7	21.55	18.2

4. SYSTEM METHODOLOGY

Solar irradiance data provide information on how much of the Sun's energy strikes a surface at a location on the Earth during a particular period of time. Due to lack of measured

Table 1. Typical electrical appliances

Floor	Load type			Total power / floor
	Lights (40 W)	Fans (80 W)	Air-conditions (3 HP)	
Ground	565	36	4	34432
First	510	37	11	47978
Second	435	33	3	26754
Third	426	32	4	28552
Fourth	416	20	2	22716
Sum	2352	158	24	-
Total power	94080 W	12640 W	53712 W	160432 W

3.3 Climate Data

Strength of solar radiation is the primary consideration in selecting location for PV installation. The generated output power of a PV array is directly proportioned to the input solar radiation. So, to get an optimum design of rooftop PV system, it is important to collect the meteorological data for site under consideration. Hourly data of solar direct irradiance and ambient temperature are available for one year. Table 3 shows monthly average radiation on the horizontal surface which has obtained from Egyptian Metrological Authority for El-Minia site, Egypt. El-Minia and Upper Egypt region have an average daily direct insolation between 7.7 and 8.3 kWh/m²/day [1, 24]. It is clear from the Table 3 that solar energy in this region is very high during summer months, where it exceeds 8 kWh/m²/day, while the lowest average intensity is during December with a value of 3.69 kWh/m²/day and the actual sunshine duration is about 11 h/day. So, solar energy application is more and more considered in El-Minia and Upper Egypt as a renewable energy resource compared to conventional energy resources.

data of irradiance on tilted surfaces, mathematical models have been developed to calculate irradiance on tilted surfaces.

4.1 Monthly Best Tilt Angle

There are various types of tracker systems such as single-axis, dual-axis tracking, monthly tracking and seasonal tracking systems. The new approach presented based on monthly best tilt angle tracking. Hourly solar radiation incident upon a horizontal surface is available for many locations. However solar radiation data on tilted surfaces are generally not available [25]. The monthly best tilt angle, β (degrees) can be calculated according to the following equations[25]

$$\beta = \phi - \delta \quad (1)$$

where; ϕ (degrees)is the site latitude and δ (degrees)is the declination angle. The declination angle can be calculated for the Northern hemisphere in terms of an integer representing the recommended day of the year, n , by:

$$\delta = 23.45^\circ * \sin \left[360 * \frac{(284 + n)}{365} \right] \quad (2)$$

4.2 Calculation of Radiation on the Tilted Surfaces:

Average daily solar radiation on horizontal surface, \bar{H} for each calendar month can be expressed by defining, \bar{K}_T the fraction of the mean daily extraterrestrial radiation, \bar{H}_o as[25]:

$$\bar{K}_T = \frac{\bar{H}}{\bar{H}_o} \quad (3)$$

The average daily radiation on the tilted surface, \bar{H}_T , can be expressed as follows:

$$\bar{H}_T = \bar{R} * \bar{H} = \bar{R} * \bar{K}_T * \bar{H}_o \quad (4)$$

where; \bar{R} is the ratio between radiation on tilted surfaces to radiation on horizontal surfaces. \bar{R} can be estimated individually by considering the beam, diffuse and reflected components of the radiation incident on the tilted surfaces toward the equator. Assuming diffuse and reflected radiation can be isotropic then \bar{R} can be expressed as follows [25]:

$$\bar{R} = \frac{\bar{H}_T}{\bar{H}} = \left(1 - \left(\frac{\bar{H}_d}{\bar{H}} \right) \right) * \bar{R}_b + \left(\frac{\bar{H}_d}{\bar{H}} \right) \left(\frac{(1 + \cos(S))}{2} \right) + \rho * \left(\frac{(1 - \cos(S))}{2} \right) \quad (5)$$

$$\frac{\bar{H}_d}{\bar{H}} = 1.39 - 4.027 * \bar{K}_T + 5.531 * (\bar{K}_T)^2 - 3.108 * (\bar{K}_T)^3 \quad (6)$$

where; \bar{H}_d is the monthly average daily diffuse radiation. However \bar{R}_b , can be estimated to be the ratio of the extraterrestrial radiation on the tilted surface to that on horizontal surface for the month, thus [25]:

$$\bar{R}_b = \frac{\sin(\delta) \sin(\phi - \delta) (\pi/180) \omega'_s + \cos \delta \cos(\phi - \delta) \sin(\omega'_s)}{\sin(\delta) \sin(\phi) (\pi/180) + \cos(\delta) \cos(\phi) \sin(\omega_s)} \quad (7)$$

where;

$$\omega_s = \cos^{-1}(-\tan(\phi) \tan(\delta)) \quad (8)$$

$$\omega'_s = \min[\omega_s, \cos^{-1}(-\tan(\phi - S)) \tan(\delta)] \quad (9)$$

4.3 Calculation of Average Power for One PV Module

The complete model of PV module consists of a current source whose intensity I_{ph} (A) is directly proportional to

radiation G (kW/m²), which connected in parallel with two diodes, one that simulates the diffusion of minority charge and the other corresponding to the recombination of the junction. The parallel resistance, R_{sh} (Ω), represents the leakage current losses, and the series resistor, R_s (Ω), represents the internal losses of the cell, the heat losses by Joule effect due to current flow, impurities and losses among cell connections [26]. The two-diode equivalent electrical circuits describing the solar cells array used in the analysis are shown in Figure 3 and Figure 4[27]. The equivalent circuit of the module is arranged in series and parallel cells with N_s and N_p respectively.

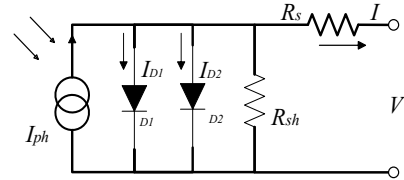


Figure 3. Two-diode circuit model of PV cell model

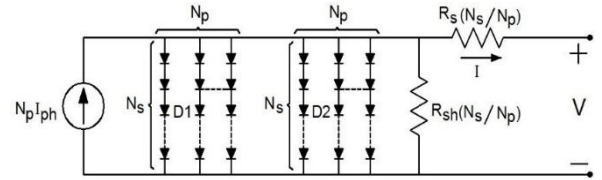


Figure 4. Equivalent circuit model of generalized PV

The characteristic equation of I-V curve is given by [28]:

$$I = I_{ph} - I_{s1} \left[\exp \left(\frac{V + I R_s}{a_1 \cdot V_T} \right) - 1 \right] - I_{s2} \left[\exp \left(\frac{V + I R_s}{a_2 \cdot V_T} \right) - 1 \right] - \left(\frac{V + I R_s}{R_{sh}} \right) \quad (10)$$

where; I_{s1} (A) is the diffusion saturated current of D_1 , I_{s2} (A) is the recombination saturated current of D_2 . I_{ph} , a function of temperature and solar insolation, is given as follows [29, 30]:

$$I_{ph} = \left(\frac{G}{G_{STC}} \right) [I_{ph \text{ at } STC} + K_i (T - T_{STC})] \quad (11)$$

where; ($G_{STC}=1\text{kW/m}^2$)is the solar irradiance at Standard Test Conditions, $I_{ph \text{ at } STC}$ (A)is the photo current at STC, K_i (A/C^o) is the short circuit current coefficient, T (K^o) is the PV cell working temperature, T_{STC} (K^o)is the PV cell at STC. The two-diode saturation currents as function of working PV temperature are given as follow [29, 30]:

$$I_{s1} = I_{s1 \text{ at } STC} \left(\frac{T}{T_{STC}} \right)^3 \exp \left[\left(\frac{q \cdot E_g}{a_1 \cdot K} \right) \left(\frac{1}{T_{STC}} - \frac{1}{T} \right) \right] \quad (12)$$

$$I_{s2} = I_{s2 \text{ at } STC} \left(\frac{T}{T_{STC}} \right)^3 \exp \left[\left(\frac{q \cdot E_g}{a_2 \cdot K} \right) \left(\frac{1}{T_{STC}} - \frac{1}{T} \right) \right] \quad (13)$$

Where; q is the electron charge ($1.6 \cdot 10^{-19}$ C), K is the Boltzmann constant ($1.38 \cdot 10^{-23}$ J/K), E_g (eV)is the band gap energy of semiconductor, a_1 and a_2 are the diode ideality factors for two-diode model. The current equation of module is written as [29, 30]:

$$I = N_p I_{ph} - N_p I_{s1} \left[\exp \left(\frac{V + I R_s (N_s / N_p)}{a_1 \cdot N_s \cdot V_T} \right) - 1 \right] - N_p I_{s2} \left[\exp \left(\frac{V + I R_s (N_s / N_p)}{a_2 \cdot N_s \cdot V_T} \right) - 1 \right] - \left(\frac{V + I R_s (N_s / N_p)}{R_{sh} (N_s / N_p)} \right) \quad (14)$$

The values of the seven-parameter in Eq. (10) can be determined to obtain I-V and P-V curves of the PV model using *Newton Raphson method*[27]. The output of the solar cell module can be calculated by the following equation:

$$P_{pv,out}(t) = V(t) * I(t) \quad (15)$$

Depending on the manufacturing process, most of PV modules can be of three types Mono-crystalline Silicon, Polycrystalline Silicon and Amorphous Silicon. Two different Silicon solar cell technologies (Mon-crystalline and Polycrystalline) with five different selected types of commercially available PV modules (i.e.190W, 270W, 305W, 350W and 420W) have been used in the proposed approach as shown in Table 4.

Table 4. Technical Characteristics of the selected PV solar modules

Module Item	Mitsubishi PV-UD190MF5	Suntech STP270S-24/Vb	ET MODULE ET-P672305WB/WW	1Sol Tech 1STH-350-WH	Solar panel Heliene 96M 420
P_{max}	190 W	270 W	305 W	350 W	420 W
V_{OC}	30.8 V	44.8 V	45.12 V	51.5 V	60.55 V
I_{sc}	8.23 A	8.14 A	8.78 A	8.93 A	9.0 A
V_{mpp}	24.7 V	35.0 V	37.18 V	43.0 V	49.53 V
I_{mpp}	7.71 A	7.71 A	8.21 A	8.13 A	8.48 A
Dimensions, m	1.658*0.834	1.956*0.992	1.956*0.992	1.652*1.306	1.967*1.310
Efficiency	13.7 %	15 %	15.72 %	16.2 %	16.4 %
Number of cells	50 cell	72 cell	72 cell	80 cell	96 cell
Cell type (Silicon)	Polycrystalline	Mono-crystalline	Polycrystalline	Mon-crystalline	Mon-crystalline
Price/unit	\$340	\$753	\$305	\$525	\$420

4.4 Calculation of Average Power for One PV Module

The number of subsystems, N_{sub} depends on the inverter rating, $P_{inverter}$ and size of PV system, P_{system} . To determine the number of subsystems, inverter rating and module data must be known.

$$N_{sub} = \frac{P_{system}}{P_{inverter}} \quad (16)$$

Series and parallel combination of each PV subsystem can be adjusted according to not only the MPP voltage range but also maximum DC input current of the inverter. Estimation of the initial total number of PV modules for each subsystem can be calculated as follows:

$$N_{PV_sub_i} = \frac{P_{inverter}}{P_{max}} \quad (17)$$

Most manufacturers of inverters for photovoltaic systems make a wide range between the maximum and minimum values of MPP voltage range (V_{mpp_max} , V_{mpp_min}), where inverters act properly and has no problem to find the maximum power point in where the module is working. Minimum and the maximum number of PV modules that can be connected in series in each branch, N_{s_min} and N_{s_max} respectively, are calculated according to the MPP voltage range as follows

$$N_{s_min} = ceil \left(\frac{V_{mpp_min}}{V_{mpp}} \right) \quad (18)$$

$$N_{s_max} = ceil \left(\frac{V_{mpp_max}}{V_{mpp}} \right) \quad (19)$$

where; V_{mpp} is the maximum power point of PV module. The optimal number of series modules, N_{s_sub} is located in the range of

$$N_{s_min} < N_{s_sub} < N_{s_max}$$

Minimum and the maximum number of PV modules that can be connected in parallel in each subsystem, N_{p_min} and N_{p_max} respectively, are calculated as follows:

$$N_{p_min} = ceil \left(\frac{N_{PV_sub_i}}{N_{s_max}} \right) \quad (20)$$

$$N_{p_max} = ceil \left(\frac{N_{PV_sub_i}}{N_{s_min}} \right) \quad (21)$$

where optimal number of parallel modules N_{p_sub} is located in the range of

$$N_{p_min} < N_{p_sub} < N_{p_max}$$

Number of PV modules connected in parallel N_{p_sub} may be set to N_{p_min} but cannot be set to N_{p_max} , because the DC current results from all parallel strings may be higher than the

maximum DC input of the inverter which may damage the inverter. For each number of series modules, N_{s_sub} in the series range calculated previously, estimation of the corresponding parallel modules for each subsystem can be calculated as follows:

$$N_{p_sub} = \text{ceil}\left(\frac{N_{PV_sub_i}}{N_{s_sub}}\right) \quad (22)$$

Then, recalculate the total number of PV module, N_{PV_sub} according to each resulted series and parallel combination

$$N_{PV_sub} = N_{s_sub} \cdot N_{p_sub} \quad (23)$$

Assuming that inverter is operating in the MPP voltage range, the operating input voltage and current of the inverter (V_{mpp_sub}, I_{mpp_sub}) can be calculated as follow:

$$V_{mpp_sub} = N_{s_sub} \cdot V_{mpp} \quad (24)$$

$$I_{mpp_sub} = N_{p_sub} \cdot I_{mpp} \quad (25)$$

From previous calculations, a database containing probable series and parallel combinations, PV modules, DC input

voltage and current for each subsystem is formed. Optimal total number of PV modules for each subsystem is selected according to minimum number of PV modules which satisfies not only the MPP voltage range but also the maximum DC input current of the inverter. The total number of PV modules, N_{PV} for the selected site can be calculated from the following

$$N_{PV} = N_{sub} \cdot N_{PV_sub} \quad (26)$$

4.5 Inverter Selection

Inverters are a necessary component in a PV system generation used to convert direct current output of a PV array into an alternating current that can be utilized by electrical loads. There are two categories of inverters, the first category is synchronous or line-tied inverters, which are used with utility connected PV systems. While the second category is stand alone or static inverters, which are designed for independent utility free power systems and are appropriate for remote PV installation. Five different types of commercially available line-tied inverters (i.e. 10 kW, 20 kW, 25 kW, 50 kW and 100 kW) have been used associated with capital costs as revealed in Table 5.

Table 5. Characteristics of the different inverter ratings

Inverter Specification	GCI-10k-LV	Sunny Tripower 20000TL	ST25000TL	HS50K3	HS100K3
Manufacturer	B&B Power co. Ltd.	SMA Solar Technology	B&B Power co. Ltd.	Han's Inverter & Grid Tech. co. Ltd.	Han's Inverter & Grid Tech. co. Ltd.
$P_{inverter}$	10.2 kW	20.45 kW	26.5 kW	55 kW	110 kW
Max. DC current	30 A	36 A	32 A	122 A	245 A
MPP voltage range	150~500 V	580~800 V	450~800 V	450~800 V	450~820 V
Max. AC power	10 kW	20 kW	25 kW	50 kW	100 kW
Max. AC current	25 A	29 A	40 A	80 A	160 A
Frequency	50/60 Hz	50 Hz	50/60 Hz	50 Hz	50 Hz
Price/unit	\$1500	\$3870	\$2650	\$8060	\$14500

4.6 Economic Feasibility

The most critical factors in determining the value of energy generated by PV system are the initial cost of the hardware and installation, and the amount of energy produced annually [31]. Commonly calculated quantities are simple payback and cost of energy (COE). A 100 kW grid connected PV system is economically feasible only if its overall earnings exceed its overall costs within a time period up to the lifetime of the system. The time at which earnings equals cost is called the payback time.

4.6.1 Cost of Electricity (COE)

The economical aspect is crucial for PV systems because of their high cost, which is reflected on price of energy produced by them. COE is a measure of economic feasibility, and when it is compared to the price of energy from other sources (primarily the utility company) or to the price for which that energy can be sold, it gives an indication of feasibility [32].

Initial capital investment cost is the sum of the investment cost of parts of PV system, i.e. PV array, DC/AC inverter and miscellaneous cost (Wiring, conduit, connectors, PV array support and grid interconnection).

$$C_{cap} = C_{PV} + C_{inverter} + C_m \quad (27)$$

Miscellaneous cost, C_m can be determined as follows:

$$C_m = C_{labor} + C_{wiring} + C_{racks} + C_{grid} \quad (28)$$

The COE (\$/kWh) is primarily driven by the installed cost and annual energy production of system, AEP which can be calculated from the following equation:

$$COE = \frac{C_{cap} + C_{main}}{AEP} \quad (29)$$

4.6.2 Simple Payback Time (SPBT)

A PV system is economically feasible only if its overall earnings exceed its overall costs within a time period up to the lifetime of the system. A simple payback time (SPBT)

provides a preliminary judgment of economic feasibility. SPBT calculation includes the value of money, borrowed or lost interest, and annual operation and maintenance costs can be calculated as follow [31].

$$SPBT = \frac{C_{cap}}{AEP * P - C_{cap} * i - C_{main}} \quad (30)$$

Economic parameters considered in the proposed rooftop grid connected PV system as shown in Table 6.

Table 6. Economic parameters considered for the proposed system

Description	Value	Notes
Installation labor cost (\$/hour) [33]	16.66	0.43 hr./unit
Installation Materials cost [Wiring, conduit, connectors] (\$/module)[33]	3.60	
Mounting structure cost (\$/Wp) [34]	0.080	
O&M costs,(\$/year)[35]	425.60	
Grid Interconnect cost (\$) [33]	2,000	
Life time, <i>N</i> (years)	25	
Tracking system	Monthly	

4.6.3 Simple Payback Time (SPBT)

Concerning to the environmental effects that can be avoided by using PV systems. CO₂ emission is the main cause of greenhouse effect, so that the total amount of CO₂ at the atmosphere must be minimized in order to reduce the global warming. Amount of tCO₂, can be calculated according to the following equation

$$CO_{2(emission)} = F_E * AEP * N \quad (31)$$

5. APPLICATIONS AND RESULTS

A new computer program has been developed based on above methodology for design and economic analyses of grid connected PV system. Flowchart of proposed MATLAB computer program is shown in Figure 5. The total load demand of the faculty is about 160.432 kW as shown from Table 2. However, these loads do not work all at one time, on the contrary working for a short time. Assuming demand load of 60% of the total load demand, so a capacity of 100 kW rooftop grid connected PV system is proposed. According the Egyptian legalization, the feed-in rates vary depending on usage. Households will receive 84.8 piaster/kWh, commercial producers will receive 90.1 piaster/kWh (under 200 kW) and 97.3 piaster/kWh for producers of 200 kW to 500 kW [36]. Rooftop PV system operational lifetime period has been set to 25 years, which is equal to guaranteed operational lifetime period of PV module. According to Ref. [35], an hourly salary of \$26.60 for a facility services engineer to maintain the system is considered. The projected maintenance costs will be 16 hours per year (\$425.60) for a medium system (less than 100 kW). Also to mount the panels on the roof, a solar panel rail kit is applied. The rail kit is sized based on the assumption that PV modules will be mounted on the roof inclined with monthly best tilt angle to optimize the energy output.

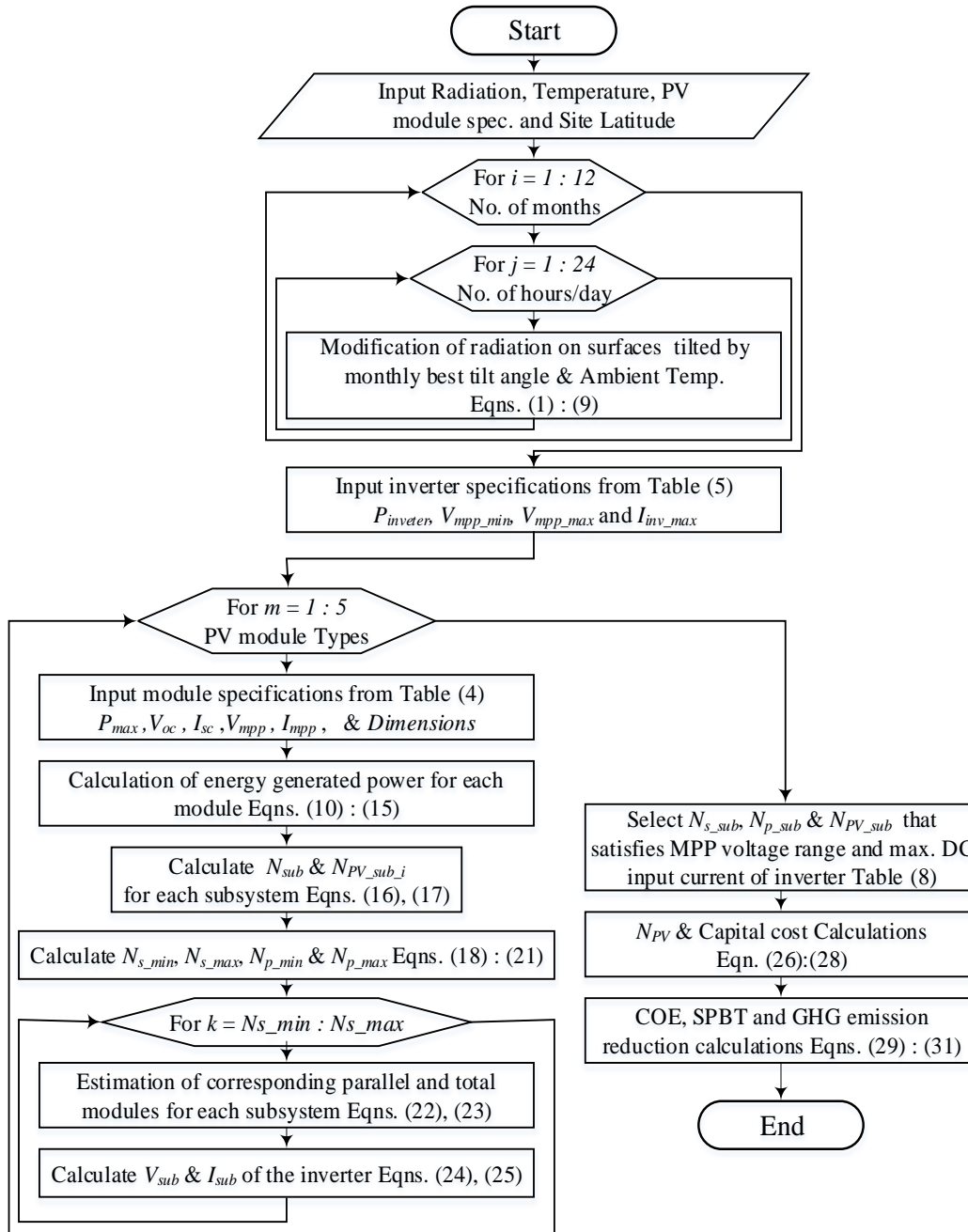


Figure 5. Procedure of proposed computer program

5.1 Configurations of PV modules for each subsystem

The first outputs of the proposed computer program are the optimum total number of PV modules for each subsystem, N_{PV_sub} , number of modules per strings N_{s_sub} , number of strings, N_{p_sub} , and finally the output voltage and current of each subsystem. Table 7 shows details configuration for each subsystem without subsystems with ST25000TL inverter where the common feature of selected PV modules is that, they have a high current at different voltage level to supply a high power with a minimum installation area which make ST25000TL inverter is not suitable for this application. Not all inverters are suitable for all applications. Power output is usually the main factor, but there are many other factors like MPP voltage range and maximum DC input current.

The electric characteristics of the PV module depend mainly on the irradiance received by the module and the module temperature. Figure 6 displays the electrical characteristics of selected module at different levels of irradiance and constant temperature for month of July. The amount of energy generated by the solar PV panel depends on peak sun hours available where peak sun hours vary throughout the year. It is clear that the change in irradiance has a strong effect on the output power of the module, but negligible effect on the open-circuit voltage. Also, it can be seen that the maximum power generated during a day in July occurs at 1:00 PM to 2:00 PM as shown in Figure 6

Table 7. Specifications for each subsystem

Inverter type	Type Details	Mitsubishi PV-UD190MF5	Suntech STP270S-24/Vb	ET MODULE ET-P672305WB/WW	1Sol Tech 1STH-350-WH	Solar panel Heliene 96M 420	
GCI-10k-LV	10 subsystem	N_{s_sub}	18	13	12	10	9
		N_{p_sub}	3	3	3	3	3
		N_{PV_sub}	54	39	36	30	27
		V_{sub}	444.6 V	455.0 V	446.16 V	430.0 V	445.77 V
		I_{sub}	23.13 A	23.13 A	24.63 A	24.39 A	25.44 A
Sunny Tripower 20000TL	5 subsystem	N_{s_sub}	27	19	17	15	17
		N_{p_sub}	4	4	4	4	3
		N_{PV_sub}	108	76	68	60	51
		V_{sub}	666.9 V	665.0 V	632.06 V	645.0 V	842.01 V
		I_{sub}	30.84 A	30.84 A	32.84 A	32.52 A	25.44 A
HS50K3	2 subsystem	N_{s_sub}	29	17	13	16	11
		N_{p_sub}	10	12	14	10	12
		N_{PV_sub}	290	204	182	160	132
		V_{sub}	716.3 V	595.0 V	483.34 V	688.0 V	544.83 V
		I_{sub}	77.1 A	92.52 A	114.94 A	81.30 A	101.76 A
HS100K3	1 subsystem	N_{s_sub}	20	17	19	15	11
		N_{p_sub}	29	24	19	21	24
		N_{PV_sub}	580	408	361	315	264
		V_{sub}	494.0 V	595.0 V	706.42 V	645.0 V	544.83 V
		I_{sub}	223.59 A	185.04 A	155.99 A	170.73 A </td <td>203.52 A</td>	203.52 A

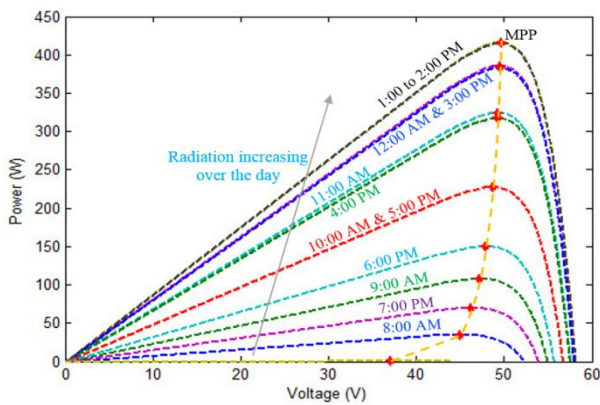


Figure 6. PV curve of Solar panel Heliene 96M 420 over day times in July

5.1.1 Optimal configuration as a detailed calculations

Many calculations have been done for many subsystems. A database containing probable series and parallel combinations, PV modules for each subsystem and DC input voltage and current is formed. Detailed calculations for optimal configuration of selected module (Heliene 96M 420) and inverter (GCI-10k-LV) based on minimum price of kWh generated can be done as follows. Input data are given in Table 4, Table 5 and Table 6

$$N_{sub} = \text{ceil} \left(\frac{P_{system}}{P_{inverter}} \right) = \text{ceil} \left(\frac{100000}{10200} \right) = \text{ceil}(9.8039) = 10 \text{ subsystems}$$

$$N_{PV_sub_i} = \text{ceil} \left(\frac{P_{inverter}}{P_{max}} \right) = \text{ceil} \left(\frac{10200}{420} \right) = \text{ceil}(24.2857) \cong 25 \text{ modules}$$

$$N_{s_min} = \text{ceil}\left(\frac{V_{mpp_min}}{V_{mp}}\right) = \text{ceil}\left(\frac{150}{49.53}\right) = \text{ceil}(3.0284) \\ \cong 4 \text{ modules}$$

$$N_{s_min} = \text{ceil}\left(\frac{V_{mpp_min}}{V_{mp}}\right) = \text{ceil}\left(\frac{500}{49.53}\right) = \text{ceil}(10.0948) \\ \cong 11 \text{ modules}$$

Optimal number of series modules N_{s_sub} is located in the following range as shown in column 2 from Table 8

$$4 < N_{s_sub} < 11$$

$$N_{p_min} = \text{ceil}\left(\frac{N_{PV_sub_i}}{N_{s_max}}\right) = \text{ceil}\left(\frac{25}{11}\right) = \text{ceil}(2.2727) \\ = 3 \text{ modules}$$

$$N_{p_max} = \text{ceil}\left(\frac{N_{PV_sub_i}}{N_{s_min}}\right) = \text{ceil}\left(\frac{25}{4}\right) = \text{ceil}(6.25) \\ = 7 \text{ modules}$$

Optimal number of parallel modules N_{p_sub} is located in the following range as shown in column 3 from Table 8

$$3 < N_{p_sub} < 7$$

$$N_{p_sub} = \text{ceil}\left(\frac{N_{PV_sub_i}}{N_{s_sub}}\right) = \text{ceil}\left(\frac{25}{9}\right) = \text{ceil}(2.7777) \\ = 3 \text{ modules}$$

$$N_{PV_sub} = N_{s_sub} \cdot N_{p_sub} = 9 \cdot 3 = 27 \text{ modules}$$

Assuming that the inverter is operating in the MPP voltage range, the operating input voltage and current of the inverter can be calculated as follows as shown in columns 5 and 7 in Table 8 respectively:

$$V_{mp_sub} = N_{s_sub} \cdot V_{mp} = 9 \cdot 49.53 = 445.77 \text{ V}$$

$$I_{mp_sub} = N_{p_sub} \cdot I_{mp} = 3 \cdot 8.48 = 25.44 \text{ A}$$

Each 9 modules will be connected in series to build 3 parallel strings. Considering open circuit voltage ($V_{oc} = 60.55 \text{ V}$) and short circuit current ($I_{sc} = 9.0 \text{ A}$) of Heliene 96M 420 solar module at standard conditions, the open circuit voltage and short circuit current for resultant PV array.

$$V_{oc_array} = 60.55 \cdot 9 = 544.95 \text{ V}$$

$$I_{oc_array} = 9 \cdot 3 = 27 \text{ A}$$

Which also satisfy the voltage and current limits of selected inverter. MPP voltage range of the (GCI-10k-LV) inverter is 150-500 V, As can be seen from Table 8, all configurations can be implemented according to operating voltage except the last one (case 8) because the voltage exceeds the maximum value of MPP voltage range. On the other hand, maximum DC input current of selected inverter is 30 A, so cases 1 to 5 from Table 8 cannot be implemented which resultant current higher than maximum DC input current of selected inverter. Although the minimum number of PV modules for a subsystem is 25 as revealed in column 4 in Table 8, this number is not the optimal number of PV modules for a subsystem because the resultant current is 42.4 A, which is higher than the maximum DC input current of the inverter (30 A). Optimal total number of PV modules for each subsystem is selected according to minimum number of PV modules which satisfies not only MPP voltage range but also maximum DC input current of the inverter. So the optimal number of PV modules from the remaining cases 6 and 7 is 27 modules.

The total number of PV modules can be calculated from the following equation as shown in Table 9:

$$N_{PV} = N_{sub} \cdot N_{PV_sub} = 10 \cdot 27 = 270 \text{ modules}$$

Table 8. Optimal Configuration of PV module and inverter

Case	N_{s_sub}	N_{p_sub}	N_{sub}	V_{sub}	Voltage condition	I_{sub}	Current condition	Optimal
1	4	7	28	198.12 V	Satisfied	59.36 A	Not Satisfied	
2	5	5	25	247.65 V	Satisfied	42.40 A	Not Satisfied	
3	6	5	30	297.18 V	Satisfied	42.40 A	Not Satisfied	
4	7	4	28	346.71 V	Satisfied	33.92 A	Not Satisfied	
5	8	4	32	396.24 V	Satisfied	33.92 A	Not Satisfied	
6	9	3	27	445.77 V	Satisfied	25.44 A	Satisfied	Selected
7	10	3	30	495.30 V	Satisfied	25.44 A	Satisfied	
8	11	3	33	544.83 V	Not Satisfied	25.44 A	Satisfied	

Table 9. Optimal total number of PV modules for each system

Module Inverter	Mitsubishi PV-UD190MF5	Suntech STP270S-24/Vb	ET MODULE ET-P672305WB/WW	1Sol Tech 1STH-350-WH	Solar panel Heliene 96M 420
N_{PV} GCI-10k-LV	540	390	360	300	270

Sunny Tripower 20000TL	540	380	340	300	255
HS50K3	580	408	364	320	264
HS100K3	580	408	361	315	264

5.1.2 Why ST25000TL inverter is not suitable for this application?

ST25000TL inverter is not selected where the output DC current of subsystems exceed the maximum DC input current of the inverter according to the following calculations

$$N_{PV_{sub_i}} = \text{ceil}\left(\frac{P_{inverter}}{P_{max}}\right) = \text{ceil}\left(\frac{26500}{420}\right) = \text{ceil}(63.0952) \cong 64 \text{ modules}$$

$$N_{s_{min}} = \text{ceil}\left(\frac{V_{mpp_{min}}}{V_{mpp}}\right) = \text{ceil}\left(\frac{450}{49.53}\right) = \text{ceil}(9.0854) \cong 10 \text{ modules}$$

$$N_{s_{min}} = \text{ceil}\left(\frac{V_{mpp_{min}}}{V_{mpp}}\right) = \text{ceil}\left(\frac{800}{49.53}\right) = \text{ceil}(16.1518) \cong 17 \text{ modules}$$

Optimal number of series modules $N_{s_{sub}}$ is located in the following range as shown in column 2 from Table 10:

$$10 < N_{s_{sub}} < 17$$

$$N_{p_{min}} = \text{ceil}\left(\frac{N_{PV_{sub_i}}}{N_{s_{max}}}\right) = \text{ceil}\left(\frac{64}{10}\right) = \text{ceil}(6.4000) \cong 7 \text{ modules}$$

$$N_{p_{max}} = \text{ceil}\left(\frac{N_{PV_{sub_i}}}{N_{s_{min}}}\right) = \text{ceil}\left(\frac{64}{17}\right) = \text{ceil}(3.7647) \cong 4 \text{ modules}$$

Optimal number of parallel modules $N_{p_{sub}}$ is located in the following range as shown in column 3 from Table 10:

$$4 < N_{p_{sub}} < 7$$

$$N_{p_{sub}} = \text{ceil}\left(\frac{N_{PV_{sub_i}}}{N_{s_{sub}}}\right) = \text{ceil}\left(\frac{64}{10}\right) = \text{ceil}(6.4) \cong 7 \text{ modules}$$

Assuming that the inverter is operating in the MPP voltage range, the operating input voltage and current of the inverter can be calculated as follows as shown in columns 4 and 6 in Table 10 respectively:

$$V_{mp_{p_{sub}}} = N_{s_{sub}} \cdot V_{mpp} = 10 * 49.53 = 495.3 \text{ V}$$

$$I_{mp_{p_{sub}}} = N_{p_{sub}} \cdot I_{mpp} = 7 * 8.48 = 59.36 \text{ A}$$

Notice that DC output current of subsystem (59.36 A) is higher than the maximum DC input of the inverter (32 A) which makes ST25000TL inverter not suitable for this application as revealed in Table 10 and Table 11.

Detailed calculations of subsystems with ST25000TL inverter which is not suitable for the proposed rooftop grid connected PV systems are shown in Table 11, where case in column 2 from Table 11 refers to the number of probable system configurations with each module type.

Table 10. Subsystems with ST25000TL inverter and Heliene 96M 420 PV module

Case	$N_{s_{sub}}$	$N_{p_{sub}}$	N_{sub}	V_{sub}	Voltage condition	I_{sub}	Current Condition	Optimal
1	10	7	70	495.30 V	Satisfied	59.36 A	Not Satisfied	There is no optimal configuration
2	11	6	66	544.83 V	Satisfied	50.88 A	Not Satisfied	
3	12	6	72	594.36 V	Satisfied	50.88 A	Not Satisfied	
4	13	5	65	643.89 V	Satisfied	42.40 A	Not Satisfied	
5	14	5	70	693.42 V	Satisfied	42.40 A	Not Satisfied	
6	15	5	75	742.95 V	Satisfied	42.40 A	Not Satisfied	
7	16	4	64	792.48 V	Satisfied	33.92 A	Not Satisfied	
8	17	4	68	842.01 V	Not Satisfied	33.92 A	Not Satisfied	

Table 11. ST25000TL inverter under different PV modules

Module type	Case	$N_{s_{sub}}$	$N_{p_{sub}}$	N_{sub}	V_{sub}	I_{sub}	Condition
Mitsubishi	Start (1)	19	8	152	469.30 V	61.68 A	Not Satisfied

PV-UD190MF5	End (15)	33	5	165	815.10 V	38.55 A	Not Satisfied
Suntech STP270S-24/Vb	Start (1)	13	8	104	455.00 V	61.68 A	Not Satisfied
	End (11)	23	5	115	805.00 V	38.55 A	Not Satisfied
ET MODULE ET-P672305WB/WW	Start (1)	13	7	91	483.34 V	57.47 A	Not Satisfied
	End (10)	22	4	88	817.96 V	32.84 A	Not Satisfied
ISol Tech 1STH-350-WH	Start (1)	11	7	77	473.00 V	56.91 A	Not Satisfied
	End (9)	19	4	76	817.00 V	32.52 A	Not Satisfied
Heliene 96M 420	Start (1)	10	7	70	495.30 V	59.36 A	Not Satisfied
	End (8)	17	4	68	842.01 V	33.92 A	Not Satisfied

Finally, layout of the PV system illustrated in Figure 7. The PV system is mainly composed of 270 Heliene 96M 420 mono-crystalline silicon PV modules. The PV modules are arranged in 3 parallel strings, with 9 series modules in each. A power diode, called bypass diode, connected in parallel with each individual module or a number of modules. The function of this diode is to conduct the current when one or more of these modules are damaged or shaded. Another diode, called blocking diode, is usually connected in series with each string to prevent reverse current flow and protect the modules. Each subsystem is connected to GCI-10k-LV inverter which has the feature of controlling the MPP of PV array through a built-in DC/DC converter.

Failure of one distributed inverter does not stop the operation of the entire PV system, because they operate separately. The generated AC power from the inverter is injected into the grid and/or utilized by the local loads.

5.2 Economic Calculations

Using data from Tables 4, Table 5 and Table 6 and results from Table 7 and Table 9, economic calculation of PV system can be done. Solar PV array is the most expensive component in the proposed system where system cost is determined primarily by the cost of PV modules as shown in Figure 8. Thus, most of the research activities performed in this area are concerned with manufacturing low-cost solar cells with acceptable efficiencies. In the proposed approach, batteries are not considered, so the capital cost is reasonable.

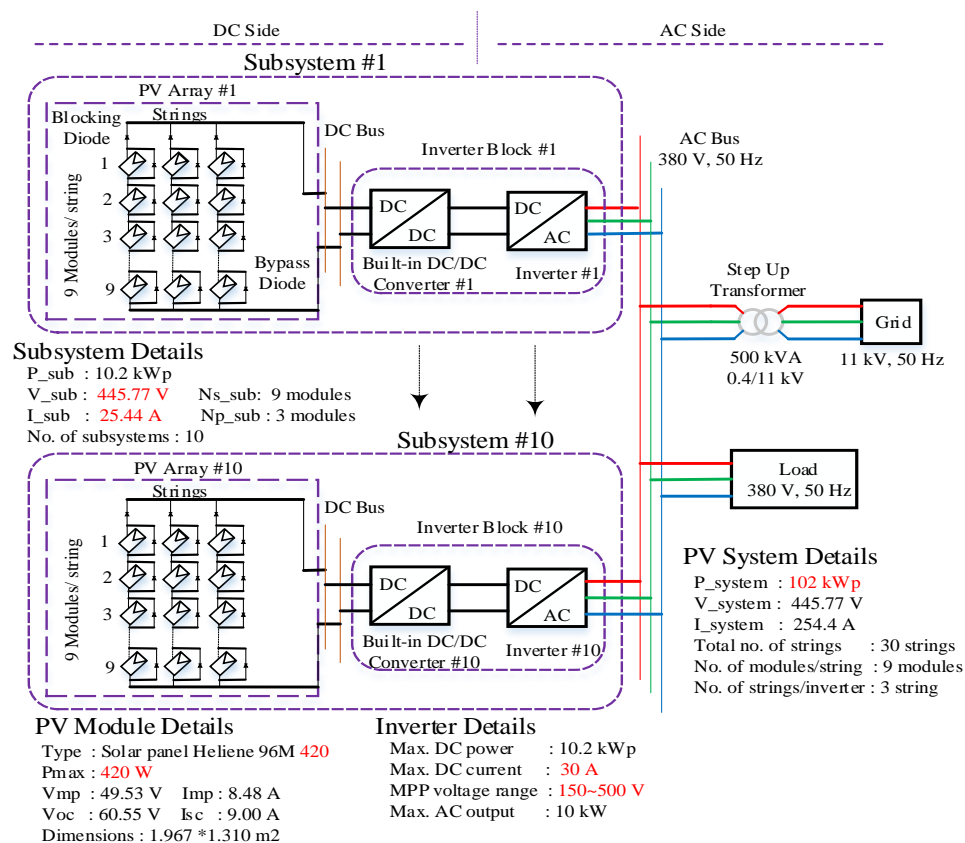


Figure 7. Rooftop grid-connected PV system description

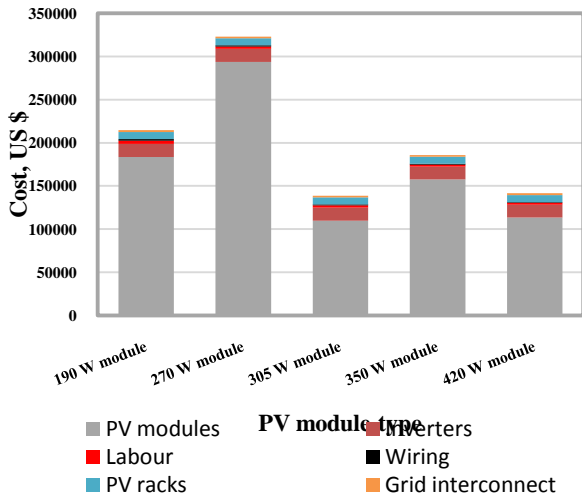


Figure 8. Cost analysis for GCI-10k-LV inverter under different types of PV modules

5.3 AEP, Cash Flows and COE Calculations

Fig. 9 shows generated power for each PV module over the year. From this figure, monthly generated energy can be calculated according to Table 7 as shown in Figure 10. AEP and corresponding cash inflows resulting from electric energy generated purchased to the electric grid for each configuration of PV system are calculated in Table 12. From this table, it can be seen that, the maximum generated energy from GCI-10k-LV with ten subsystem is equal to 258.8006 MWh, while yearly electrical energy purchased to electric grid is equal to \$32427.71, meanwhile the optimal system configuration consists of PV module (Heliene 96M 420) and inverter (GCI-10k-LV) based on minimum cost of kWh generated which is equal to 0.5466 \$/kWh. The cost of energy COE can be determined from eq. (29) as follows:

$$COE = \frac{C_{cap} + C_{main}}{AEP \left(\frac{kWh}{year} \right)} = \frac{\$141466.226 + \$425.6}{258800.6} = 0.5482 \$/kWh$$

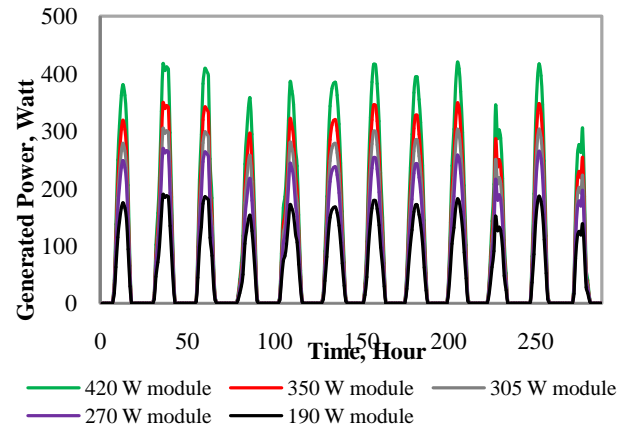


Figure 9. Generated power for each PV module over the year

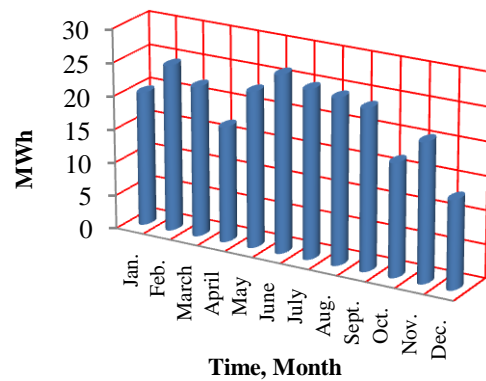


Figure 10. Monthly generated PV power for the proposed system

5.4 SPBT estimation

SPBT for the rooftop grid connected PV system can be calculated according to eq. (30). The cost of proposed rooftop grid connected PV system can be recouped in 6.958 years, where systems with larger PV output always achieve a shorter payback period due to the lower cost

$$SPBT = \frac{C_{cap}}{AEP * P - C_{cap} * i - C_{main}} = \frac{141466.226}{258.8006 * 10^3 * 0.1253 - 141466.226 * 0.0825 - 425.6} = 6.958 \text{ years}$$

Table 12. AEP, selling price and COE

Parameter	Module	Mitsubishi	Suntech	ET MODULE	ISol Tech	Solar panel
	Inverter	PV-UD190MF5	STP270S-24/Vb	ET-P672305WB/WW	1STH-350-WH	Heliene 96M 420
AEP (MWh/yr.)	GCI-10k-LV	228.8893	234.6086	206.5385	238.2875	258.8006
	Sunny Tripower 20000TL	228.8893	228.5928	195.0641	238.2875	244.4227
	HS50K3	245.8443	245.4365	208.8333	254.1732	253.0494
	HS100K3	245.8443	245.4365	207.1121	250.2018	253.0494

	GCI-10k-LV	28679.82	29396.45	25879.27	29857.42	32427.71
Selling price (\$/yr.)	Sunny Tripower 20000TL	28679.82	28642.67	24441.53	29857.42	30626.16
	HS50K3	30804.29	30753.19	26166.81	31847.90	31707.08
	HS100K3	30804.29	30753.19	25951.14	31350.28	31707.08
	GCI-10k-LV	0.9374	1.3768	0.6721	0.7801	0.5482
COE (\$/kWh)	Sunny Tripower 20000TL	0.9565	1.3988	0.7017	0.7984	0.5702
	HS50K3	0.9370	1.3793	0.6792	0.7804	0.5557
	HS100K3	0.9304	1.3727	0.6725	0.7756	0.5493
	GCI-10k-LV	0.9374	1.3768	0.6721	0.7801	0.5482

5.5 GHG emissions reduction

The emission factor, F_E is set to be 0.699 kg CO_{2-eq}/kWh [37]. Annual GHG reduction income for a rooftop PV system is calculated using prices for tCO₂ reduction credits. Prices for CO₂ reduction credits differ based on many factors such as how the credit is generated and how it will be delivered. The model estimates that the PV system reduces GHG emissions by 180.9016 tons of CO_{2-eq} annually. About 4522.54 tons of CO₂ emissions will be avoided as the rooftop grid connected PV system replaces the need of some electricity from the existing power grid. At an assumed emission cost factor of about US\$30/ton CO₂ as in Ref. [38], the emissions of 0.699 kg CO₂/kWh give a CO₂-revenue of 2.097 cent/kWh (15.07 piaster/kWh). Annual CO₂ emission reduction

$$CO_{2(emission)} = F_E * AEP$$

$$= 0.699 \left(\frac{kg \ CO_{2-eq}}{kWh} \right) * 258.8006$$

$$* 10^3 (kWh) = 180.9016 \ t \frac{CO_{2-eq}}{year}$$

CO₂ emission reduction during the lifetime of the project

$$CO_{2(emission)} = F_E * AEP * N$$

$$= 0.699 \left(\frac{kg \ CO_{2-eq}}{kWh} \right) * 258.8006$$

$$* 10^3 (kWh) * 25 (years)$$

$$= 4522.54 \ t \ CO_{2-eq}$$

6. CONCLUSION

In this paper, a new approach for optimum design of rooftop grid connected PV system has been proposed to be install in Faculty of Engineering as a case study. From results obtained above, the followings are the salient conclusions that can be drawn from this paper:

1. A MATLAB computer program has been proposed for new design approach of rooftop grid connected PV system installation for a given input data.
2. The best type of PV module was found solar panel Heliene 96M 420 and GCI-10k-LV inverter type with ten subsystems and 27 module in each.
3. Annual energy production of about 258.8 MWh with total annual GHG emissions reduction of

180.9016 tons of CO₂ can be avoided from entering the local atmosphere each year.

4. Total cost for producing one kWh of electricity is estimated to be 0.5482 cents/kWh.
5. Cost of rooftop PV system can be recouped in 6.958 years using SPBT calculations.
6. Not all inverters are suitable for all applications, where ST25000TL inverter cannot be used in this system due to its low DC input current.
7. The presented study would be useful and applicable for planning rooftop grid-connected PV installations in any other geographical region location once the input data are gathered.

7. REFERENCES

- [1] R. Y. Georgy and A. T. Soliman, 2007. Mediterranean and national strategies for sustainable development priority field of Action 2: energy and climate change, energy efficiency and renewable energy, *Egypt's National Study, Final Report, Plan Bleu, Regional Activity Centre*.
- [2] Ministry of Electricity and Energy, New and Renewable Energy Authority (NREA), *Annual Report 2010/2011*.
- [3] Hong Soo Goh, 2011. "The effect of grid operating conditions on the harmonic performance of grid-connected PV inverters," Ph.D. Thesis, School of Electrical, Electronic & Computer Engineering, Newcastle University.
- [4] A. Al-Salaymeh, Z. Al-Hamamre, F. Sharaf, and M. R. Abdelkader, "Technical and economical assessment of the utilization of photovoltaic systems in residential buildings: the case of Jordan," *Energy Conversion and Management*, Vol. 51, No. 8, pp. 1719-1726, August 2010.
- [5] P. E. Posedly, 2008. Modelling and analysis of photovoltaic generation and storage systems for residential use, M.Sc. Thesis, Department of Electrical and Computer Engineering, College of Engineering, University of Cincinnati.
- [6] R. Banos, F. Manzano-Agugliaro, F. G. Montoya, C. Gil, A. Alcayde, and J. Gomez, "Optimization methods applied to renewable and sustainable energy: A review,"

- Renewable and Sustainable Energy Reviews*, vol. 15, no. 4, pp. 1753-1766, May 2011.
- [7] A. S. Bahaj, "Photovoltaic roofing: issues of design and integration into buildings," *Renewable Energy*, Vol. 28, No. 14, pp. 2195–2204, November 2003.
- [8] E.D. Mehleri, H. Sarimveis, N.C. Markatos, and L.G. Papageorgiou, "Optimal design and operation of distributed energy systems: Application to Greek residential sector," *Renewable Energy*, Vol. 51, pp. 331-342, March 2013.
- [9] D C. O. C. Oko, E. O. Diemuodeke, E. O. Omuakwe, and E. Nnamdi, "Design and economic analysis of a photovoltaic system: a case study," *International Journal of Renewable Energy Development (IJRED)*, Vol. 1, No. 3, pp. 65-73, August 2012.
- [10] H. H. El-Tamaly and A. A. Elbaset, "Performance and economic study of interconnected PV system with electric utility accompanied with battery storage," in, *11th International Middle East Power Systems Conference, MEPCON'2006, IEEE*, pp. 328-333, 2006.
- [11] DA. Fernandez-Infantes, J. Contreras, and J. L. Bernal-Agustin, "Design of grid connected PV systems considering electrical, economical and environmental aspects: a practical case," *Renewable Energy*, Vol. 31, No. 13, pp. 2042-2062, October 2006.
- [12] H. Suryoatmojo, A. Elbaset, A. Syafaruddin, and T. Hiyama, "Genetic Algorithm Based Optimal Sizing of PV-Diesel-Battery System Considering CO₂ Emission and Reliability," *International Journal of Innovative Computing Information and Control*, Vol. 6, No. 10, pp. 4631-4649, October 2010.
- [13] X. Gong and M. Kulkarni, "Design optimization of a large scale rooftop photovoltaic system," *Solar Energy*, Vol. 78, No. 3, pp. 362-374, March 2005.
- [14] H. Ren, W. Gao, and Y. Ruan, "Economic Optimization and Sensitivity Analysis of Photovoltaic System in Residential Buildings," *Renewable Energy*, Vol. 34, No. 3, pp. 883-889, March 2009.
- [15] J. C. Hernández, P. G. Vidal, and G. Almonacid, "Photovoltaic in grid-connected buildings, sizing and economic analysis," *Renewable Energy*, Vol. 15, No. 1, pp. 562-565, September 1998.
- [16] J. Samimi, E. A. Soleimani, and M. S. Zabihi, "Optimal sizing of photovoltaic systems in varied climates," *Solar Energy*, Vol. 60, No. 2, pp. 97-107, February 1997.
- [17] R. Haas, M. Ornetzeder, K. Hametner, A. Wroblewski, and M. Hubner, "Socio-economic aspects of the Austrian 200 kWp photovoltaic-rooftop program," *Solar Energy*, Vol. 66, No. 3, pp. 183-191, June 1999.
- [18] N. K. Bansal and S. Goel, "Integration of photovoltaic technology in cafeteria building, at Indian Institute of Technology, New Delhi," *Renewable Energy*, Vol. 19, No. 1, pp. 65-70, January 2000.
- [19] A. Mellit, S. A. Kalogirou, L. Hontoria, and S. Shaari, "Artificial Intelligence Techniques for Sizing Photovoltaic Systems: A review," *Renewable and Sustainable Energy Reviews*, Vol. 13, No. 2, pp. 406-419, February 2009.
- [20] W. Muneer, K. Bhattacharya, and C. A. Cañizares, "Large-Scale Solar PV Investment Models, Tools, and Analysis: The Ontario Case," *IEEE Transaction on Power Systems*, Vol. 26, No. 4, pp. 2547-2555, April 2011.
- [21] DKornelakis A, Koutroulis E., "Methodology for The Design Optimization and The Economic Analysis of Grid-connected Photovoltaic Systems," *IET Transactions on Renewable Power Generation*, Vol. 3, No. 4, pp. 476-492, December 2009.
- [22] Kornelakis A, Marinakis Y., "Contribution for Optimal Sizing of Grid-connected PV-Systems Using PSO," *Renewable Energy*, Vol. 35, No. 6, pp. 1333-1341, June 2010.
- [23] A. Kornelakis, "Multiobjective Particle Swarm Optimization for the optimal design of photovoltaic grid-connected systems," *Solar Energy*, Vol. 84, No. 12, pp. 2022-2033, December 2010.
- [24] A. Tsikalakis, T. Tomtsi, N. D. Hatziaargyriou, A. Poullikkas, C. Malamatenios, E. Giakoumelos, O. C. Jaouad, A. Chenak, A. Fayek, and T. Matar, "Review of best practices of solar electricity resources applications in selected Middle East and North Africa (MENA) countries," *Renewable and Sustainable Energy Reviews*, Vol. 15, No. 6, pp. 2838-2849, August 2011.
- [25] S. A. Klein, "Calculation of Monthly Average Insolation on Tilted Surfaces," *Solar Energy*, Vol. 19, No. 4, pp. 325-329, 1977.
- [26] F. Adamo, F. Attivissimo, and M. Spadavecchia, "A tool for photovoltaic panels modeling and testing," in *Instrumentation and Measurement Technology Conference, 2010 IEEE*, pp. 1463-1466, 2010.
- [27] Adel A. Elbaset, H. Ali, and M. Abd-El Sattar, "Novel seven-parameter model for photovoltaic modules," *Solar Energy Materials and Solar Cells*, Vol. 130, pp. 442-455, 2014.
- [28] J.A. Gow, C.D. Manning, "Development of a photovoltaic array model for use in power-electronics simulation studies," *IEE Proceedings on Electric Power Applications*, Vol. 146, pp. 193–199, March 1999.
- [29] Huan-Liang Tsai, Ci-Siang Tu and Yi-Jie Su, "Development of generalized photovoltaic model using MATLAB/SIMULINK," in *Proceedings of the world congress on Engineering and computer science, WCECS 2008*, San Francisco, USA, pp. 1-6, 2008.
- [30] K. Ishaque, Z. Salam, and H. Taheri, "Accurate MATLAB Simulink PV system simulator based on a two-diode model," *Journal of Power Electronics*, Vol. 11, No. 2, pp. 179-187, March 2011.
- [31] Foster, M. Ghassemi, and A. Cota, *Solar energy: renewable energy and the environment*: CRC Press, 2009.
- [32] D. B. Nelson, M. H. Nehrir, and C. Wang, "Unit sizing and cost analysis of stand-alone hybrid wind/PV/fuel cell power generation systems," *Renewable Energy*, Vol. 31, No. 10, pp. 1641-1656, August 2006.
- [33] Alan Goodrich, Ted James, and Michael Woodhouse, "Residential, Commercial, and Utility-Scale Photovoltaic (PV) System Prices in the United States: Current Drivers

and Cost-Reduction Opportunities,” *Technical Report*, NREL/TP-6A20-53347, National Renewable Energy Laboratory, February 2012.

- [34] <http://www.ensolar.com/pv/mounting-system-datasheet/549> [Accessed May, 2014].
- [35] P. Eiffert and A. Thompson, “U.S. Guidelines for the Economic Analysis of Building-Integrated Photovoltaic Power Systems,” *Technical Report*, NREL/TP-710-25266, National Renewable Energy Laboratory, February 2000.
- [36] PV magazine, Photovoltaic Markets and Technology website available from <http://www.pv-magazine.com/news/details/beitrag/egypt-announces-renewableenergy-feed-in-tariffs100016525/#axzz3OqfgDWHo>[Accessed October, 2014].
- [37] P. Arun, R. Banerjee and S. Bandyopadhyay, “Optimum sizing of battery integrated diesel generator for remote electrification through design –space approach,” *Energy*, Vol. 33, No. 7, pp. 1155-1168, July 2008.
- [38] SR. W. Wies, R. A. Johnson, A. N. Agrawal, and T. J. Chubb, “Simulink model for economic analysis and environmental impacts of a PV with diesel-battery system for remote villages,” *IEEE Transactions on Power Systems*, vol. 20, pp. 692-700, 2005.